ELSEVIER

Thermochimica Acta 364 (2000) 173–179

thermochimica acta

www.elsevier.com/locate/tca

Vesicle — α-amino acid and vesicle–amide interactions: effects of added α-amino acids and amides on gel to liquid–crystal transitions for four aqueous vesicular systems

Michael J. Blandamer[a,*], Barbara Briggs[a], Paul M. Cullis[a], Keith D. Irlam[a], Jan B.F.N. Engberts[b], Lisette Streefland[b]

[a]*Department of Chemistry, University of Leicester, Leicester LE1 7RH, UK*

[b]*Physical Organic Chemistry Unit, Stratingh Institute, University of Groningen, Nijenborgh 7, 9747 AG Groningen, The Netherlands*

Received 9 August 2000; accepted 18 August 2000

Abstract

Interactions of α-amino acids, glycine (gly), valine (val), leucine (leu) and phenylalanine (phe) and the closely related phenylalaninamide (phea) with cationic vesicles formed by dimethyldioctadecylammonium bromide (DOAB), dihexadecyldimethylammonium bromide (DHAB), with anionic vesicles formed by sodium ditetradecyl phosphate (DTP) and with zwitterionic vesicles formed by dimyristoyl (C14:0) phosphatidylcholine (DMPC) have been probed using differential scanning microcalorimetry (DSC). Gel-to-liquid transitions for DTP, DOAB, DHAB and DMPC vesicular systems are relatively unaffected by added α-amino acids. In contrast added phea markedly changes the recorded scans for DSC for DTP and DMPC vesicular systems indicating that small changes in the structure of added solutes can have dramatic effects on the structures and thermal characteristics of the vesicles in aqueous suspensions. The results indicate, perhaps surprisingly, that α-amino acids are not incorporated into the bilayers whereas phea is incorporated into DTP and DMPC bilayers. © 2000 Elsevier Science B.V. All rights reserved.

Keywords: α-Amino acids; Cationic vesicles; Anionic vesicles; DMPC; DSC; Bilayers

1. Introduction

Essential biochemical functions are associated with the structural properties of biological cell membranes [1–3]. Proteins, sugars, glycolipids and cholesterol are located in phospholipid bilayers resulting in a complex supramolecular assembly and making it difficult to study properties of cell membranes directly. Simple synthetic vesicles [4–7] have many features in common with cell membranes and offer a useful basis for chemical aspects of probing membrane systems [8]. Naturally-occurring α-amino acids exist in living organisms in both their free forms and in condensed forms as peptides and proteins [9]. The object of this study was to probe the nature of the interaction between α-amino acid residues found in the peptides and proteins with natural bilayers and model bilayer systems in an attempt to understand the processes involved in the penetration and disruption of bilayer structures.

The α-amino acids used were gly, val, leu and phe; see Scheme 1. In aqueous solution between pH ca. 3

* Corresponding author. Tel.: +44-116-252-2140; fax: +44-116-252-3789.
E-mail address: mjb@le.ac.uk (M.J. Blandamer).

0040-6031/00/$ – see front matter © 2000 Elsevier Science B.V. All rights reserved.
PII: S0040-6031(00)00647-X

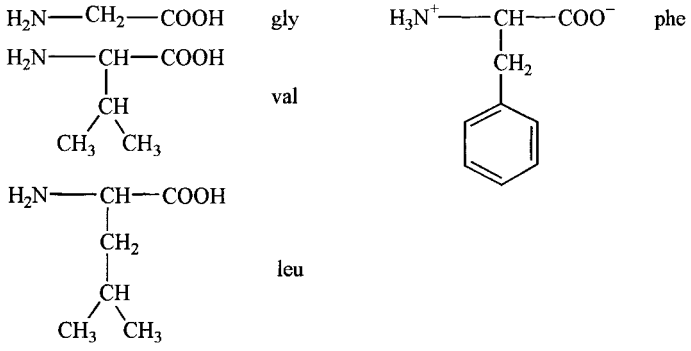

Scheme 1.

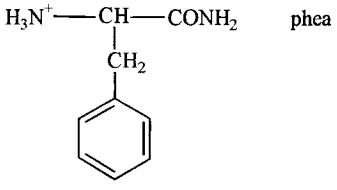

Scheme 2.

and 9 α-amino acids are predominantly present as zwitterions. We also used the closely-related cationic amide, phea (Scheme 2) to probe its interaction with bilayers. Four different types of synthetic vesicles (Scheme 3) were chosen to investigate the impact of oppositely-charged headgroups on their interaction with the α-amino acids and the amide.

Using DSC, a chain-packing transition can be characterised for vesicles formed by DTP, DOAB, DHAB and DMPC [10]. Three important parameters describe these transitions: (1) the transition or melting temperature T_m; (2) the patch number describing the number of monomers in the bilayer co-operatively undergoing the transition and (3) the enthalpy of transition per monomer. The "hot water" method was used to prepare the vesicular suspensions [10].

Previously, we reported [11] evidence of vesicle–surfactant interactions based on scans recorded by

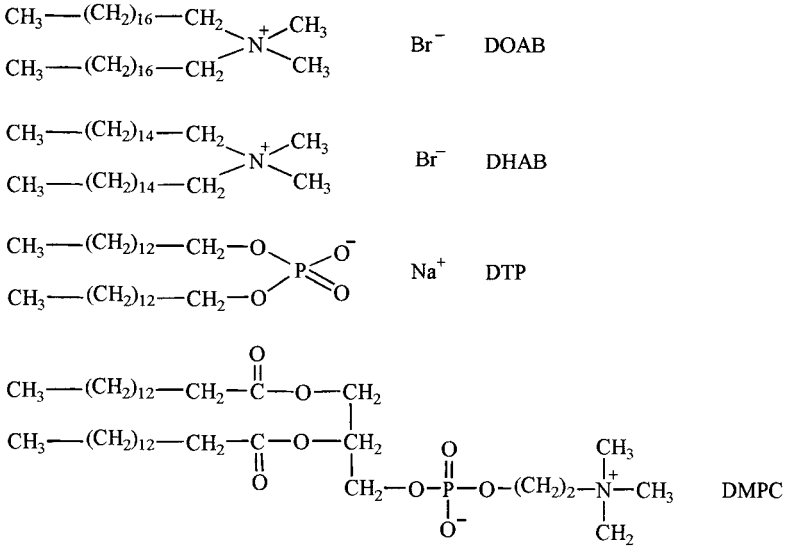

Scheme 3.

DSC for suspensions of both DOAB and DDP when sodium *n*-dodecyl sulfate (SDS), sodium dodecyl phosphate (SDP) or hexadecyltrimethylammonium bromide (CTAB) are added. The major impact on the thermal stability of the bilayers was attributed to the charged head group. Here, we report the importance of headgroup interactions on the molecular match/mismatch between differently charged vesicular suspensions and their guest α-amino acids or amide. We show how a small change in the structure of the guest molecule has a dramatic impact on bilayer chain packing.

2. Experimental

2.1. Materials

Preparation of DTP has been described [10]. DOAB, DHAB (Aldrich) and DMPC (Sigma) were used as purchased.

To prepare DOAB, DHAB, DTP and DMPC suspensions, a weighed amount of the solid was added to a known volume of buffer to produce the required concentration of 2×10^{-3} mol dm^{-3}. The buffer solution contained 5×10^{-3} mol dm^{-3} Hepes [*N*-(2-hydroxyethyl) piperazine-*N*-(2-ethane sulfonic acid)] and 5×10^{-3} mol dm^{-3} sodium ethanoate and was adjusted to pH 7.4. The aqueous suspensions were heated to (a) ca. 50°C for DOAB (aq) and DHAB (aq) solutions; and (b) ca. 60°C for DTP (aq) and DMPC (aq) solutions. The aqueous systems were held at these temperatures for 30 min while being stirred. The suspensions were then allowed to cool to room temperature.

A known mass of either α-amino acid or amide was added to the cooled vesicle suspension. The solutions were stirred until the additive had dissolved, placed in the sample cell of the calorimeter and scanned in the appropriate temperature range several times either after immediate cooling to low temperature, or after standing at low temperature for 11 h.

The scanning temperature range was 15–80°C for DOAB (aq), 5–70°C for DHAB (aq), 20–80°C for DTP (aq containing gly, val, leu or phe), 3–70°C for DTP (aq containing phea) and 10–70°C for DMPC (aq). The concentrations of α-amino acid or amide used with each vesicular suspension were 8×10^{-3}, 5×10^{-2}, 1×10^{-1} and 1.5×10^{-1} mol dm^{-3} giving a vesicle surfactant to α-amino acid (or amide) concentration ratio of 1:4, 1:25, 1:50 and 1:75.

2.2. Calorimetry

A MicroCal differential scanning microcalorimeter was used to record the heat capacities of the vesicular suspensions relative to an aqueous solution containing no bilayer system [10]. The volume of the cell was 1.2 cm^3 and the temperature scan rate was 60°C h^{-1}. The derived property is the differential heat capacity δC_p as a function of temperature. A previously recorded water–water baseline is subtracted from each recorded scan for the vesicular systems.

In the textbook case, a maximum in δC_p can be understood in terms of a two-state equilibrium of the form X⇌Y characterised by equilibrium constant K at temperature T and the standard enthalpy of reaction; Eq. (1).

$$C_{pm}(T) = \left[\frac{(\Delta_m H^0)^2}{R \cdot T^2}\right] \frac{K}{(1+K)^2} \quad (1)$$

The maximum in $C_{pm}(T)$ occurs at the temperature where K is unity, the plot of $C_{pm}(T)$ against T having a bell-shape. Analysis of DSC scans for vesicular systems presents a problem where the underlying process is effectively a phase transition from a gel state to a liquid–crystal state, the maximum of the recorded plot being the phase transition temperature, characteristic of a given vesicular system. Below their phase transition temperature (gel state), the vesicular bilayers contain thousands of surfactant monomers packed in a regular array with no local mobility. When a given vesicular system is heated the surfactants gain local mobility at a characteristic temperature T_m. Above this transition temperature, the vesicle is in a liquid crystalline state. At the gel-to-liquid crystal transition the surfactants gain cooperatively local freedom in groups of up to several hundred surfactant monomers. These groups of surfactant monomers comprise the co-operative melting domains or patches [10]. A given vesicle comprises many of these domains in a 'patchwork quilt' arrangement. The number of monomeric surfactant molecules in each domain, the patch number, is characteristic of the vesicle. At the outset, this number is a variable in the analysis together with T_m and $\Delta_m H^0$. As an

Table 1
Parameters calculated using DSC scans for DTP, DHAB, DOAB and DMPC (2×10^{-3} mol dm^{-3}) on addition of gly, val, leu, phe and phea (1×10^{-1} mol dm^{-3})

Surfactant	Aa[a]	T_m (°C)	$\Delta_m H^0$ (kJ mol^{-1})	Patch number (n)
DTP	–	54.7 ± 0.1	23.2 ± 0.4	303 ± 14
	gly	55.1 ± 0.1	21.9 ± 0.2	409 ± 11
	val	54.2 ± 0.1	17.7 ± 0.2	373 ± 11
	leu	52.3 ± 0.1	22.4 ± 0.4	365 ± 16
	phe	51.2 ± 0.1	21.6 ± 0.1	396 ± 6
	phea	16.3 ± 0.1	36.1 ± 2.0	432 ± 61
DHAB	–	28.8 ± 0.1	27.1 ± 0.6	177 ± 10
	gly	28.8 ± 0.1	24.1 ± 0.4	200 ± 13
	val	29.1 ± 0.1	24.2 ± 0.3	364 ± 0
	leu	28.8 ± 0.1	26.0 ± 0.3	342 ± 4
	phe	28.0 ± 0.1	32.0 ± 0.2	292 ± 5
	phea	27.9 ± 0.1	28.1 ± 0.2	285 ± 5
DOAB	–	47.7 ± 0.1	39.4 ± 0.1	211 ± 1
	gly	47.7 ± 0.1	34.5 ± 0.3	290 ± 6
	val	47.8 ± 0.1	32.6 ± 0.1	332 ± 2
	leu	47.7 ± 0.1	42.9 ± 0.2	269 ± 3
	phe	46.2 ± 0.1	48.9 ± 0.3	312 ± 3
	phea	46.5 ± 0.1	34.7 ± 0.2	300 ± 5
DMPC	–	23.4 ± 0.4	21.1 ± 0.1	892 ± 9
	gly	23.5 ± 0.1	23.9 ± 0.1	879 ± 7
	val	23.6 ± 0.2	19.6 ± 0.2	791 ± 12
	leu	3.5 ± 0.1	20.8 ± 0.2	833 ± 20
	phe	23.4 ± 0.1	21.9 ± 0.4	680 ± 14
	phea	20.9 ± 0.1	19.8 ± 0.5	187 ± 15

[a] AA≡amino acid or amide.

estimated patch number is increased in the curve-fitting process so the width of the calculated bell at (C_{pm}(max)/2) decreases [10]. For each system reported here good agreement between observed and calculated scans was obtained using the patch numbers recorded in the Table 1.

3. Results

Second scans recorded for freshly prepared solutions and all subsequent scans on the same solution were reproducible for all solutions investigated. Otherwise, the first scans were significantly different from subsequent scans on the same solution. The results of the analysis of DSC scans are summarised in the Table 1.

For systems prepared using only 2×10^{-3} mol dm^{-3} DTP in buffer the characteristic melting temperature, T_m, was 54.7°C. The scans were analysed to yield a calorimetric enthalpy of transition equal to 23.2 ± 0.4 kJ (monomer mol)$^{-1}$. The co-operative melting domains or patches comprised approximately 300 monomers. A summary of the results for 2×10^{-3} mol dm^{-3} DTP suspensions to which were added separately 0.1 mol dm^{-3} val (see also Fig. 1), gly, leu, phe and phea is given in Fig. 2. The melting temperature, T_m, for DTP solutions containing gly, val, leu or phe and the associated calorimetric enthalpy of transition were hardly affected by the presence of the α-amino acids. However, in DTP suspensions containing phea there was a dramatic shift in T_m to lower temperature and the size and shape of the scan also changed dramatically. The temperature range of the transition for suspensions containing 1×10^{-1} mol dm^{-3} phea was approximately 30°C compared to approximately 7°C for DTP in buffer. This broad and shallow transition was centred at around 30°C. Similar dramatic effects were observed for the other concentrations of phea.

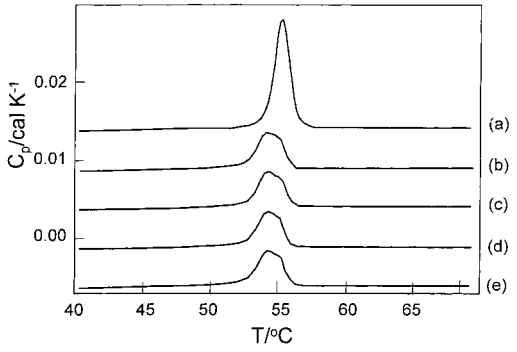

Fig. 1. Repeat scans of the dependence on temperature of differential heat capacity for DTP (aq; hepes buffer, 2×10^{-3} mol dm^{-3}) containing val (1×10^{-1} mol dm^{-3}). Scans 1, 2, 3 and 4 were recorded after immediate cooling to 20°C. Scan 5 was recorded after equilibration at 20°C for 11 h (the scans have been displaced for clarity on the heat capacity axis).

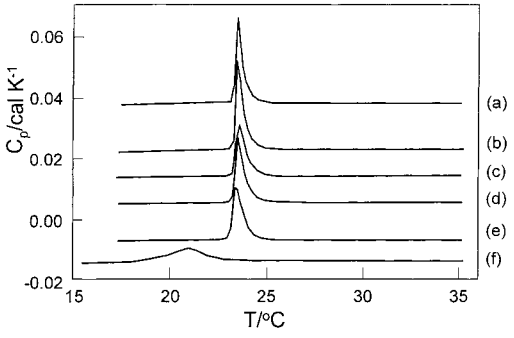

Fig. 3. Dependence on temperature of differential heat capacity for DMPC (aq; hepes buffer, 2×10^{-3} mol dm^{-3}) containing α-amino acids or amide (1×10^{-1} mol dm^{-3}): (a) no additive; (b) gly; (c) val; (d) leu; (e) phe; (f) phea (scans have been displaced for clarity on the heat capacity axis).

Similar patterns emerged when the same α-amino acids and phea were added separately to 2×10^{-3} mol dm^{-3}, DMPC suspensions (Fig. 3). The transition was almost unaffected in DMPC suspensions containing 0.1 mol dm^{-3} gly, val, leu or phe but addition of 0.1 mol dm^{-3} phea shifted T_m from 23.4 to 20.9°C and dramatically altered the shape of the recorded scan. The temperature range of transition increased from approximately 1.5 to approximately 9°C and the bell-shaped plot was much shallower. For systems prepared using only 2×10^{-3} mol dm^{-3} DMPC in buffer, the characteristic T_m was 23.4°C. The scans were analysed to yield a calorimetric enthalpy of transition equal to 21.1 ± 0.1 kJ (monomer mol)$^{-1}$ and co-operative melting domains (patches) comprising approximately 900 monomers. A similar contrast in the recorded scans was noted when α-amino acid and phea were added. In complete contrast, when the same α-amino acids and phea were added separately to 2×10^{-3} mol dm^{-3} DOAB and DHAB suspensions, no anomalous effects on the main melting transition were recorded when phea was added to the suspensions (Figs. 4 and 5).

For systems prepared using only 2×10^{-3} mol dm^{-3} DHAB in buffer the characteristic T_m was 28.8°C. The scans were analysed to yield a calorimetric

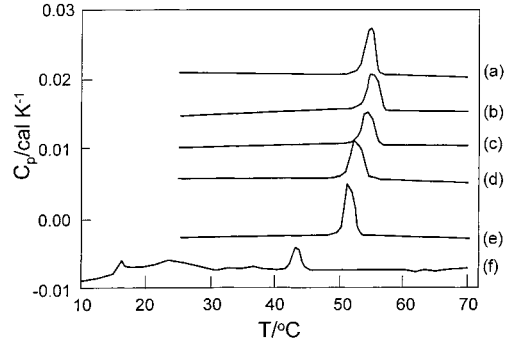

Fig. 2. Dependence on temperature of differential heat capacity for DTP (aq; hepes buffer, 2×10^{-3} mol dm^{-3}) containing α-amino acids or amide (1×10^{-1} mol dm^{-3}): (a) no additive; (b) gly; (c) val; (d) leu; (e) phe; (f) phea (scans have been displaced for clarity on the heat capacity axis).

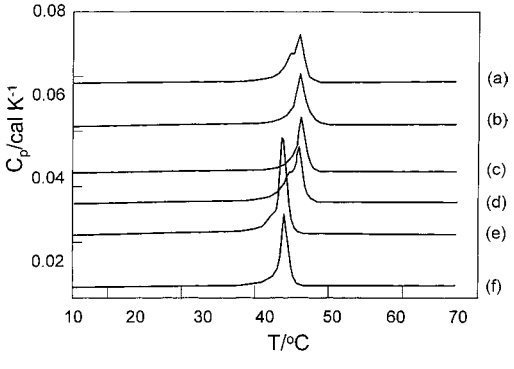

Fig. 4. Dependence on temperature of differential heat capacity for DOAB (aq; hepes buffer, 2×10^{-3} mol dm^{-3}) containing α-amino acids or amide (1×10^{-1} mol dm^{-3}): (a) no additive; (b) gly; (c) val; (d) leu; (e) phe; (f) phea (scans have been displaced for clarity on the heat capacity axis).

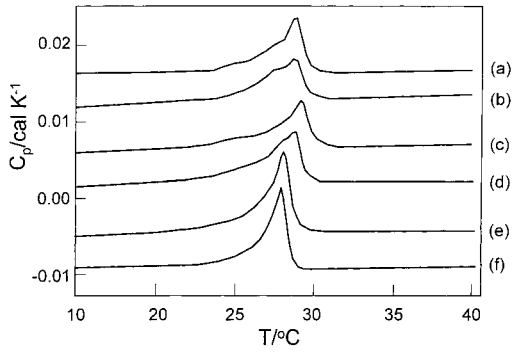

Fig. 5. Dependence on temperature of differential heat capacity for DHAB (aq; hepes buffer, 2×10^{-3} mol dm^{-3}) containing α-amino acids or amide (1×10^{-1} mol dm^{-3}): (a) no additive; (b) gly; (c) val; (d) leu; (e) phe; (f) phea (scans have been displaced for clarity on the heat capacity axis).

enthalpy of transition equal to 27.1 ± 0.6 kJ (monomer mol)$^{-1}$ and co-operative melting domains comprising approximately 180 monomers. For suspensions containing 1×10^{-1} mol dm^{-3} α-amino acids and phea, the T_m was unaffected; the calorimetric enthalpy of transition was similar but the co-operative melting domains comprised more DHAB monomers, e.g. for suspensions containing 0.1 mol dm^{-3} val the co-operative melting domains comprised approximately 350 DHAB monomers.

For systems prepared using only 2×10^{-3} mol dm^{-3} DOAB in buffer the characteristic T_m was 47.7°C. The scans were analysed to yield a calorimetric enthalpy of transition equal to 39.4 ± 1 kJ (monomer mol)$^{-1}$ and co-operative melting domains comprising approximately 200 monomers. For suspensions containing separately 0.1 mol dm^{-3} α-amino acids and phea, only small changes in T_m and calorimetric enthalpy of transition were recorded but again the cooperative melting domains grew, e.g. for suspensions containing 0.1 mol dm^{-3} val the co-operative melting domains grew from approximately 200 to 300 DOAB monomers.

4. Discussion

The DSC data for DMPC and DTP solutions to which phea was added clearly demonstrate that phea dramatically modifies the bilayers of the synthetic vesicles. By contrast, there is little evidence for interaction in solutions of DTP, DMPC, DOAB and DHAB containing the α-amino acids and for the latter two bilayers containing phea.

In the case of the DTP and DMPC bilayers, we suggest that the positively charged phea creates a molecular mismatch resulting in major changes to the molecular network when the amide molecules penetrate into the vesicles. While we rule out the possibility that the α-amino acids are incorporated into the bilayers, we do not rule out the possibility that these acids interact with the bilayers, possibly by being adsorbed on the vesicular surface. Such interaction would account for the observation that the first scans significantly differ from the second and all subsequent scans on the same solution. The equilibrium distribution of the α-amino acids is achieved when the vesicles are initially in liquid crystal form. Further heating and cooling cycles do not alter the distribution of the amino acids resulting in reproducible scan patterns.

For DHAB and DOAB bilayers containing amino acids and plea and for DTP bilayers containing amino acids, the small changes in the calorimetric enthalpy of transition yet the significant increase in the co-operative melting domains suggests that both the gel and liquid crystal phases of the vesicles have increased molecular attractions in the presence of these additives. We suggest that in the cationic bilayers of DHAB and DOAB increased head-group attractions are due to interactions between the ammonium head groups and the carbonyl group of the additives. With the anionic DTP bilayers, increased head group attractions are achieved by interaction of the phosphate head groups with the ammonium groups of the amino acids. The DSC scans indicate that addition of phea to DTP vesicles results in a complete alteration of the DTP molecular network. Patches of very different arrangements and compositions, having substantially different T_ms are created in the bilayer — hence the very large temperature range of the transition. This irregular network of patches causes the gel phase to have a much reduced thermal stability compared to pure DTP vesicular solutions.

The DSC results for DMPC and DTP systems containing phea clearly demonstrate that small changes in molecular structure of guest molecules can produce vastly different effects on bilayer structure. Only small

molecular mismatches are necessary between vesicular host surfactants and guest molecules to produce huge disruptions to the packing of molecules in bilayers. Another important finding from this study is that head group interactions between the host and guest molecules play a crucial role in determining their molecular compatibility and, consequently, the extent to which the orderly molecular structure of bilayers is altered by penetration of guest molecules.

References

[1] J.B.F.N. Engberts, D. Hoekstra, Biochem. Biophys. Acta 1241 (1995) 323.
[2] T.A.A. Fonteyn, J.B.F.N. Engberts, D. Hoekstra, in: S. Ohki (Ed.), Cell and Model Membrane Interactions, Plenum Press, New York, 1991, p. 215.
[3] S.D. Kohlwein, J. Chem. Ed. 69 (1992) 3.
[4] A. Wagenaar, L.A.M. Rupert, J.B.F.N. Engberts, D. Hoekstra, J. Org. Chem. 54 (1989) 2638.
[5] J.H. Fendler, Acc. Chem. Res. 13 (1980) 7.
[6] T. Kunitake, Angew. Chem. Int. Ed. Engl. 31 (1992) 709.
[7] A.M. Carmona-Ribeiro, Chem. Soc. Rev. 21 (1992) 209.
[8] J.H. Fendler, Membrane Mimetic Chemistry, Wiley, New York, 1982.
[9] T.H. Lilley, in: F. Franks (Ed.), Water Science Review, Vol. 5, CUP, 1990, p. 137.
[10] M.J. Blandamer, B. Briggs, P.M. Cullis, J.B.F.N. Engberts, Chem. Soc. Rev. 24 (1995) 251, and references therein.
[11] M.J. Blandamer, B. Briggs, P.M. Cullis, J.B.F.N. Engberts, A. Kacperska, J. Chem. Soc., Faraday Trans. 91 (1995) 4275.